Projected Changes in Streamflow and Sea Level Rise in the Kilchis and Miami river basins:
Summary of existing data and literature

Guillaume Mauger
Ingrid Tohver
Climate Impacts Group, UW Seattle
30 August 2013

MOTIVATION

The Nature Conservancy (TNC) is working to restore two tidal wetland properties along the Kilchis and Miami Rivers, located within the Tillamook bay in Oregon. Ultimately, the goal of these restoration efforts is to reestablish key habitats and foster a resilient ecosystem that is robust to future changes in climate. The two properties had previously been diked off from river and estuarine flow and converted to farmland – planned restoration efforts include removal of dikes and levees, restoration of river channels and floodplains, and creating suitable habitat for native species.

Sea level rise and streamflow change projections are needed to inform restoration actions at the Kilchis site and evaluate the effectiveness of existing restoration at the Miami site. Current analyses have assumed historical values for streamflow and sea level – a new assessment is needed to provide projected changes in streamflow (both monthly flows and extremes) as well as the range of projections for sea level rise.

Based on this need, TNC contracted the Climate Impacts Group (CIG) to provide an assessment of projected changes in hydrology and sea level based on existing CIG datasets and the scientific literature. This report describes the data, methods, and results involved in assessing future changes in streamflow, and provides a synthesis of existing research on sea level rise for the Pacific Northwest.

STREAMFLOW PROJECTIONS

Data and Methods

Streamflow projections require "downscaling" of coarse resolution Global Climate Model (GCM) projections to obtain estimates of climate change at scales that are relevant to decision-making. To obtain changes in hydrology, downscaled changes in climate are used to drive a hydrologic model, which produces estimates of runoff, soil moisture, evapotranspiration, and other variables that may be of more direct relevance than simple changes in temperature and precipitation.

For this project, hydrologic projections were obtained from two sources:

(1) The Columbia Basin Climate Change Scenarios Project (CBCCSP), and
(2) A regional climate model (RCM) projection obtained using the Weather Research and Forecasting (WRF) model.

These datasets are described in detail by *Hamlet et al. (2010; 2013)* and *Salathé et al. (2013)*, respectively. Both datasets are based on GCM projections from the Coupled Model Intercomparison Project, Phase 3 (CMIP3; *Meehl et al., 2007*) archive. In both cases, the result is a set of downscaled climate projections, gridded at 1/16th degree (~30 km^2) and produced at a daily time step. Projected changes in climate are used to drive the Variable Infiltration Capcacity (VIC) macroscale hydrologic model (*Liang et al., 1994; Gao et al., 2010*) to estimate the resulting changes in hydrology.

The primary difference between the two datasets is in the approach used to downscale the GCM projections. The CBCCSP dataset uses statistical downscaling, in which the statistics of GCM projections are combined with a gridded historical dataset (based on observations). In contrast, the WRF projection is a form of dynamical downscaling, in which a regional climate model is run using GCM projections as a boundary condition. Below we provide some additional detail on each dataset; additional background is provided in the appendix.

Columbia Basin Climate Change Scenarios Project (CBCCSP) dataset

The CBCCSP dataset (*Hamlet et al., 2010; 2013*) is a comprehensive set of statistically downscaled climate projections, using multiple downscaling approaches, greenhouse gas emissions scenarios, and time evolving projections of 21st century change. The dataset is based on GCM projections obtained from the Coupled Model Intercomparison Project, Phase 3 (CMIP3; *Meehl et al., 2007*), forced by the B1 (low 21st century emissions) and A1b (medium emissions) greenhouse gas emissions scenarios (*Nakićenović et al., 2000*). The 10 GCMs with the highest fidelity to Pacific Northwest climate were downscaled to produce projected changes in climate at 1/16th degree spatial resolution. Projections are evaluated for the 2040s (2030-2059) and the 2080s (2070-2099), relative to historical (1970-1999) values.

For the present analysis, results from the Hybrid Delta downscaling approach are used. The Hybrid Delta approach works by applying the projected change in the probability distribution of monthly temperature and precipitation to the historical record. This allows for the fact that the average may not change at the same rate as the extremes (e.g., warming trends might be greater for warmer months). These changes, projected by the GCM, are applied to the gridded historical dataset to obtain a perturbed time series of climate at each grid cell. The resulting time series retains the timing and sequence of weather events in the historical record, but is shifted to match the probability distribution projected by GCMs.

Weather Research and Forecasting (WRF) regional climate model simulation

The Weather Research and Forecasting (WRF) regional model was run using boundary conditions from the ECHAM5/MPI-OM global climate model (*Roeckner et al., 1999; 2003*) and SRES A1b emissions scenario. The WRF model was implemented as a regional climate model over the northwest United States at 12 km grid spacing (see *Salathé et al., 2010* and *Salathé et al., 2013* for details). The simulations for this project used nested grids at 36-km and 12-km spacing. Climate simulations are performed using 6-hourly forcing fields from the ECHAM5 GCM. The outer 36-km nest receives boundary conditions and interior nudging from the global fields; the inner 12-km nest is forced at its boundary by the outer nest. This study uses a 100-year (1970-2070) simulation with the WRF model using boundary conditions from the ECHAM5 global climate model. The model performance over the Northwest region has been extensively evaluated using simulations forced by reanalysis fields and is capable of resolving the fine scale structure of storms and their effects on precipitation in complex terrain (*Zhang et al. 2009; Dulière et al. 2011*; *Neiman et al. 2011; Warner et al. 2012*).

For this study, we use simulated WRF daily output of total precipitation, maximum and minimum temperature, and mean wind speed, and compare historical (1970-1999) to those for the 2050s (2040-2069). Although regional scale climate models represent the important topographic features of the Pacific Northwest (PNW) and the mesoscale structure of storms that control flooding in PNW rivers better than global models, RCM simulations are still subject to substantial biases resulting from deficiencies in both the global forcing fields and the regional model (*Wood et al. 2004; Christensen et al, 2008*). To obtain acceptable hydrologic simulations, these biases must be removed when using RCM results in impacts studies. In addition, to link the WRF results to the VIC hydrologic model, the simulations require additional downscaling from the 12 km WRF grid to the 1/16th degree VIC grid. Results from the WRF simulations were thus adjusted to the resolution of the CBCCSP dataset using the gridded historical dataset described by *Salathé et al.* (*2013*).

Hydrologic simulations

All scenarios were used as input into the Variable Infiltration Capacity (VIC) macroscale hydrologic model (*Liang et al., 1994; Gao et al., 2010*). The VIC model is a semi-distributed hydrologic model that solves the water and energy balance at each model grid cell – it has been extensively used in studies on topics ranging from water resources management to land-atmosphere interactions and climate change scenarios.

The VIC model simulates each grid cell independently, meaning that water is not transferred between cells during a simulation. The model is designed to be run at a resolution at which flow across cell boundaries is negligible in comparison with vertical fluxes of moisture resulting from precipitation and evaporation. Streamflow is calculated as a post-processing step. For small rain-dominant basins like the Miami and the Kilchis, daily streamflow is approximated as the sum of daily runoff at all upstream cells – this is appropriate when the flow of surface runoff through a

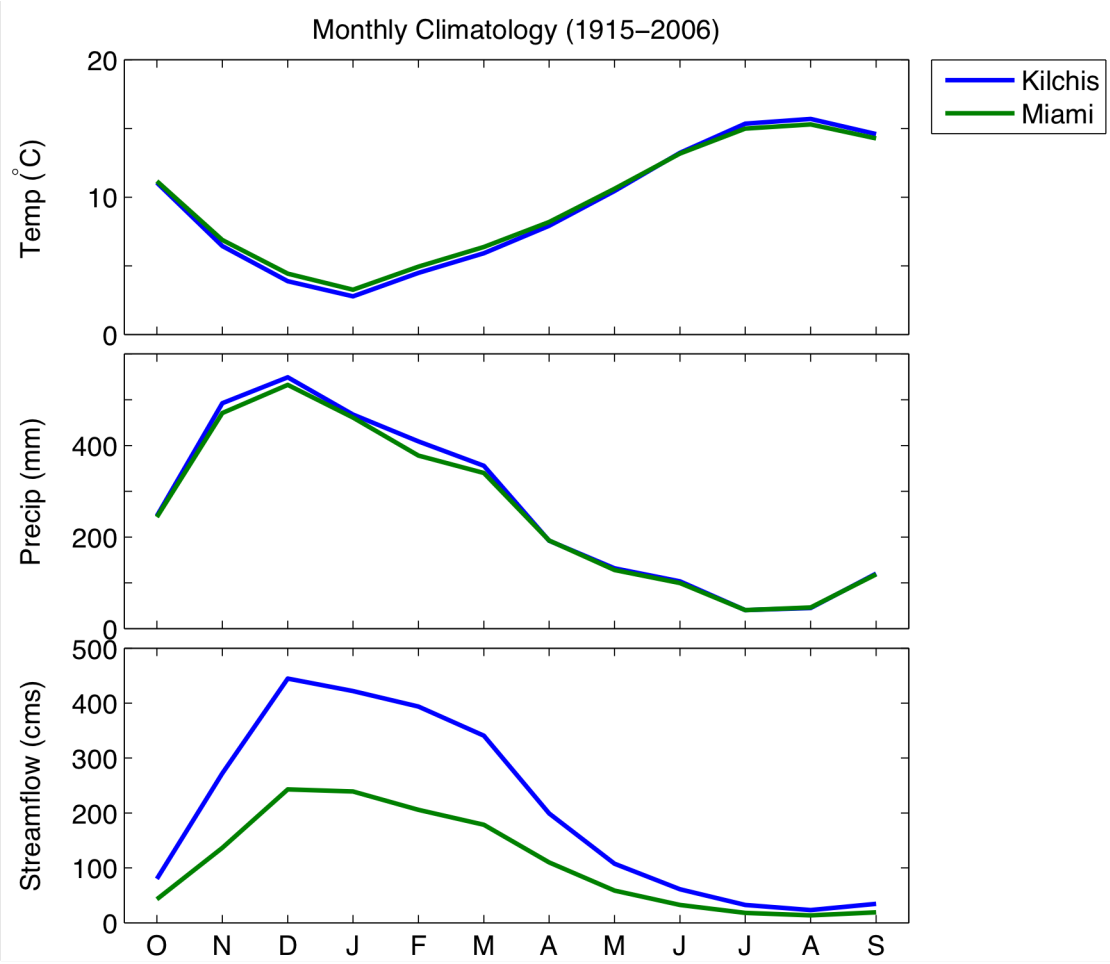

Figure 1. Monthly climatology (average for water years 1916-2006) of temperature (°C), precipitation (mm) and streamflow (cms) for the Kilchis and Miami rivers. The x-axis shows the water year as opposed to the calendar year, spanning from October ("O") to September ("S"). Precipitation and temperature stem directly from the gridded historical climate dataset, streamflow is simulated using the VIC hydrologic model.

basin is fast compared to the time scale of one day. Total basin runoff was calculated as the area-weighted sum of all 1/16th degree grid cells that overlap with the watershed. In order to minimize the impact of biases, future streamflow projections are reported in terms of the percent change relative to historical.

Assessment of Extreme flow Statistics

Extreme flow statistics – both flooding and low flows – were estimated using Generalized Extreme Value (GEV) distribution using L-moments (*Wang 1997; Hosking and Wallis 1993; Hosking 1990*) for the Kilchis and Miami basins. For flood statistics, annual peak daily flow was extracted from each water year and ranked by flow magnitude. A quantile was assigned to each ranked value using an unbiased quantile estimator (*Stedinger et al., 1993*) and then Generalized Extreme Value (GEV) distribution using L-moments was fitted to the annual maxima to estimate

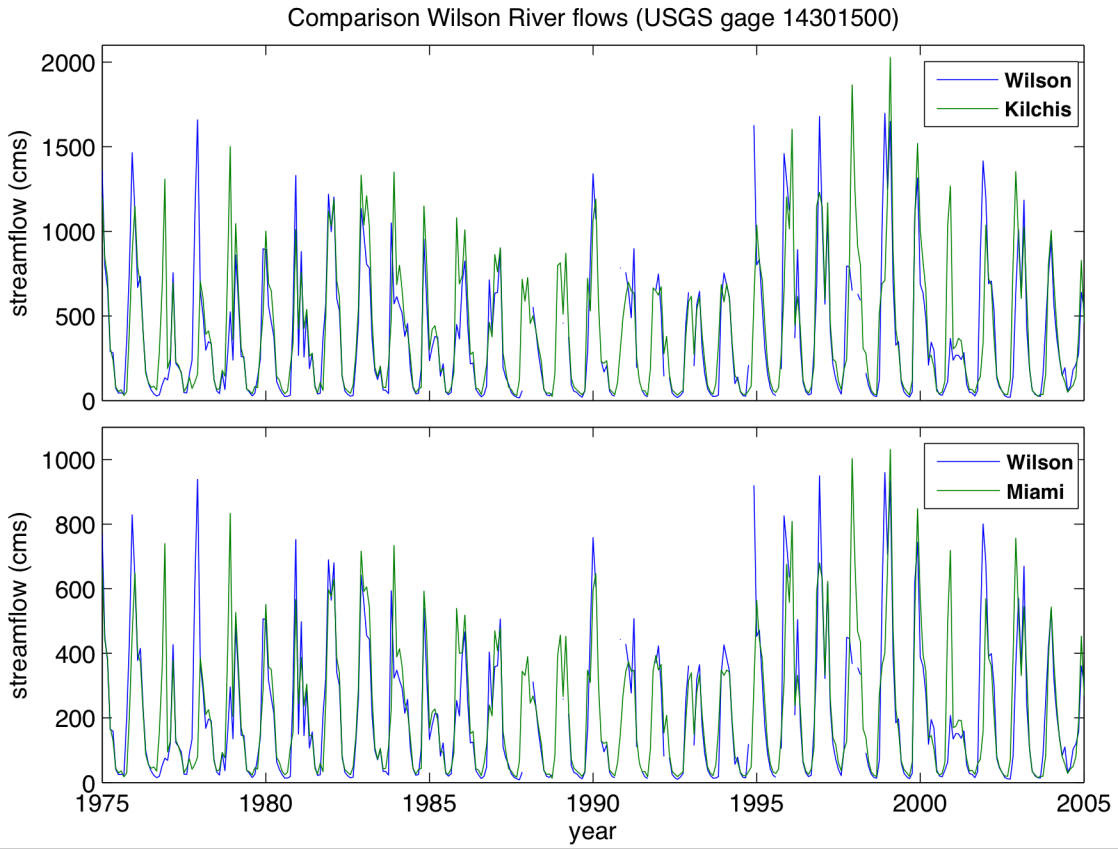

Figure 2. Comparison of simulated VIC streamflow for the Kilchis and Miami rivers with observed gage flows for the adjacent Wilson river (USGS gage number 14301500). Wilson flows have been scaled by the ratio of the basin areas to better represent anticipated flow rates for each basin. Although the records for each extend beyond these dates, only the years 1975-2005 are included for clarity.

flood magnitude with a given return interval such as the flood magnitude with 100-year return frequency (Q100) (*Wang, 1997; Hosking and Wallis, 1993; Hosking, 1990*). We report flood statistics for 2-, 5-, and 50-year recurrence intervals. Low-flow statistics were computed following a similar approach applied to the 7-day lowest flows in each water year. In this report we use the "7q10" statistic, which is the 7-day low flow with a 10-year recurrence interval. As an alternate measure of low flows, we also report the mean change in the 95% and 90% daily exceedance values for daily flows (this corresponds to the mean of the 18 and 36 lowest daily flow values in each year, respectively).

Results

Average Historical Climate

Figure 1 shows the monthly climatology – mean monthly temperature, precipitation, and streamflow – for the Kilchis and Miami river basins. These show a number of features that are typical of the mild maritime climate of the coastal northwest. First,

Table 1. Comparison of VIC monthly streamflow simulations with gage measurements at USGS gage 14301500 on the Wilson River. For the Nash-Sutcliffe (N-S) calculations, monthly streamflow from the Wilson was scaled by the ratio of the drainage areas.

	N-S	*Correlation (95% conf.)*	
		Monthly flows	*Annual flows*
Kilchis River	0.62	0.80 (0.70-0.87)	0.44 (0.22-0.62)
Miami River	0.63	0.80 (0.70-0.87)	0.45 (0.22-0.63)

temperature variations are small: winter temperatures generally stay well above freezing, and summer temperatures are mild. Second, the region receives a substantial amount of precipitation, on average totaling about 3,000 mm (119 inches) of precipitation. Third, despite being quite wet overall, summers are quite dry: 60% of all annual rainfall occurs between November and February, whereas only 10% falls between June and September.

The climatology of the two basins is reflected in the monthly streamflow hydrograph, which shows a classic rain-dominant pattern in which maximum monthly flows occur during the peak rainy season, and minimum flows occur during late summer. Although the absolute magnitude of streamflows shown for the two basins is different, this difference is simply a reflection of the different sizes of the two basins (168 km^2 for the Kilchis and 95 km^2 for the Miami). This is confirmed by the fact that simulations of the two basins show very strong covariation (correlations greater than 0.99). The strong correlations between the two indicate that the simulations do not distinguish substantially between the characteristics of the two basins – in later sections we report only the average changes for both basins, since the numbers for each individual basin are nearly identical.

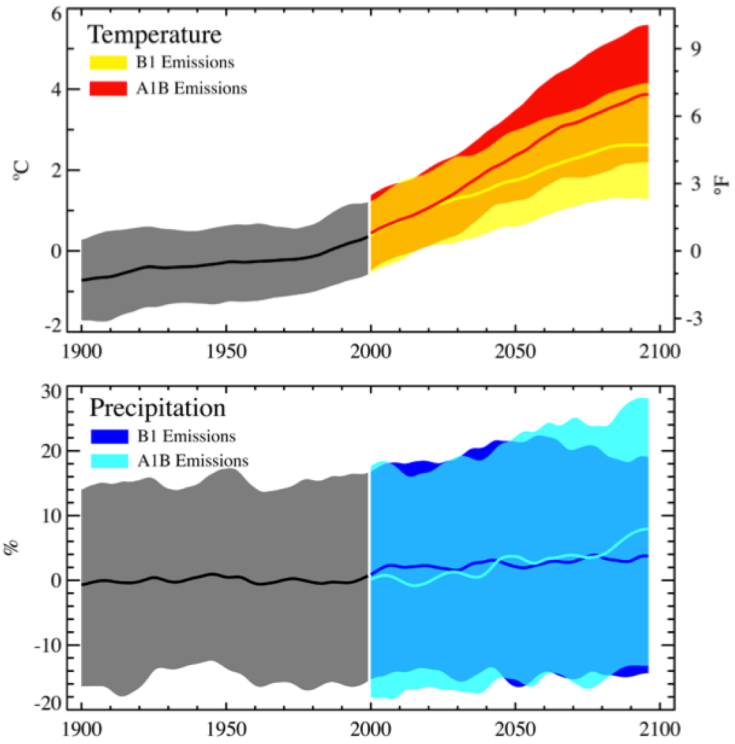

Figure 3. Time series of PNW average temperature (top, °C) and precipitation (bottom, %) for the 20th and 21st century GCM simulations. Thick lines denote the model average, smoothed with a 10-year running mean. Shaded areas show the 5th and 95th percentiles of all model values within a running 10-year window: gray shading is used for the 20th century, colored shading for the future scenarios. All values are relative to the 1970-1999 average. *Image Source: Mote and Salathé, 2010.*

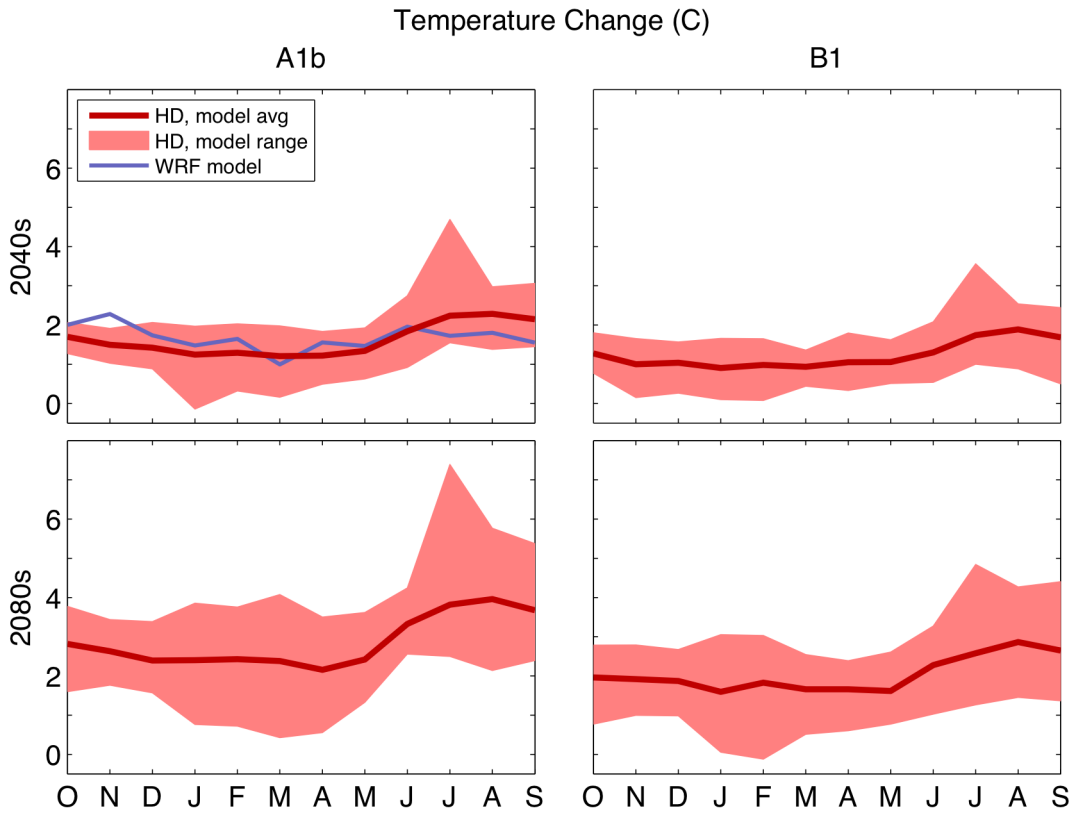

Figure 4. Projected changes in temperature (°C) for the Kilchis and Miami basins, by month. As in Figure 1, the x-axis shows the water year as opposed to the calendar year, spanning from October ("O") to September ("S"). Separate panels are shown for the A1b (left) and B1 (right) emissions scenarios, and for the 2040s (top) and 2080s (bottom). All changes are relative to 1970-1999. Note that the WRF projections are for the 2050s, not the 2040s – WRF projections do not currently exist for the B1 scenario or the 2080s.

Comparison with Observed Streamflow

There are no gage flows that are available for either the Kilchis or Miami rivers. However, gage flows do exist on the nearby Wilson river (USGS gage number 14301500), which also outlets into Tillamook bay. Figure 2 shows a comparison of the simulated monthly hydrographs for the Kilchis and Miami rivers with scaled monthly flows from the Wilson site. For each graph, the flows from the Wilson are scaled based on the ratio of basin areas (the drainage area for the Wilson gage is 417 km^2). Scaling flows by basin area assumes that meteorology (e.g., precipitation amounts) and basin characteristics are similar, and that the primary driver of differences in flows is simply the differences in the size of each catchment.

Table 1 lists the Nash-Sutcliffe coefficients, calculated using monthly flows. Since the Nash-Sutcliffe coefficient tends to emphasize absolute biases over co-variability, correlations are also listed for both monthly and annual flows. Overall these numbers indicate fair agreement between the Wilson observations and the VIC

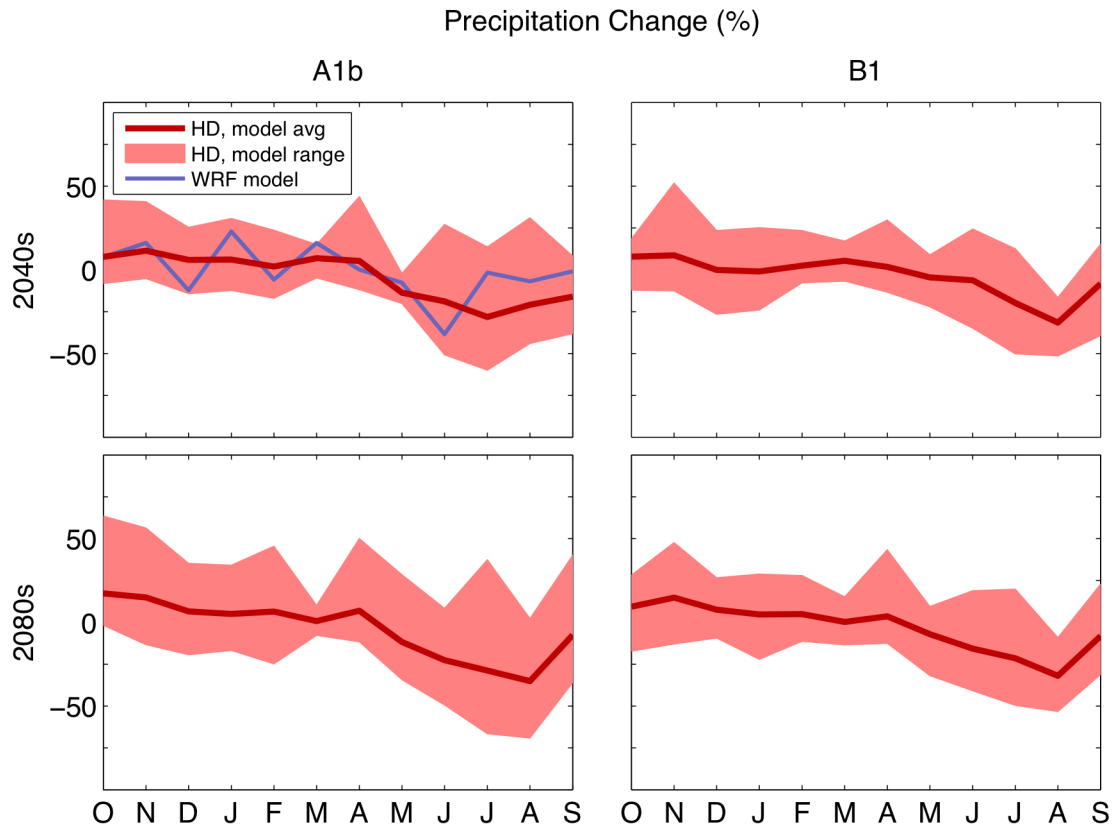

Figure 5. As in Figure 4 but showing projected changes in precipitation (%).

simulations of the Kilchis and Miami rivers, both in terms of absolute magnitude and covariability. Note that some disagreement is expected given the different size, orientation, and likely different soil and vegetation properties of the Wilson watershed relative to the Kilchis and Miami basins.

Projected changes in Temperature and Precipitation: Pacific Northwest

The time evolution of historical and mean projected changes in annual temperature (°C) and precipitation (%) for the Pacific Northwest are shown in Figure 3 (source: *Mote and Salathé, 2010*). The shaded areas show natural variability for the 20th century (gray shading) and the combination of natural variability and the range among GCM projections (colored shading). This plot highlights two key points regarding climate change in the Pacific Northwest. First, natural variability is large and can mask trends, especially over periods shorter than 30-50 years. This is an important consideration, since it means that random fluctuations in climate can result in cool years or decades despite an overall warming trend, or conversely, result in warm episodes that far exceed existing trends. Second, temperature trends are projected to be large compared to variability: changes in temperature are already apparent, and are projected to exceed the range of historical variability by about mid-century, regardless of emissions scenario. Models project fairly uniform trends for all seasons, though warming tends to be slightly greater for summer. In contrast with temperature, variability in precipitation remains large

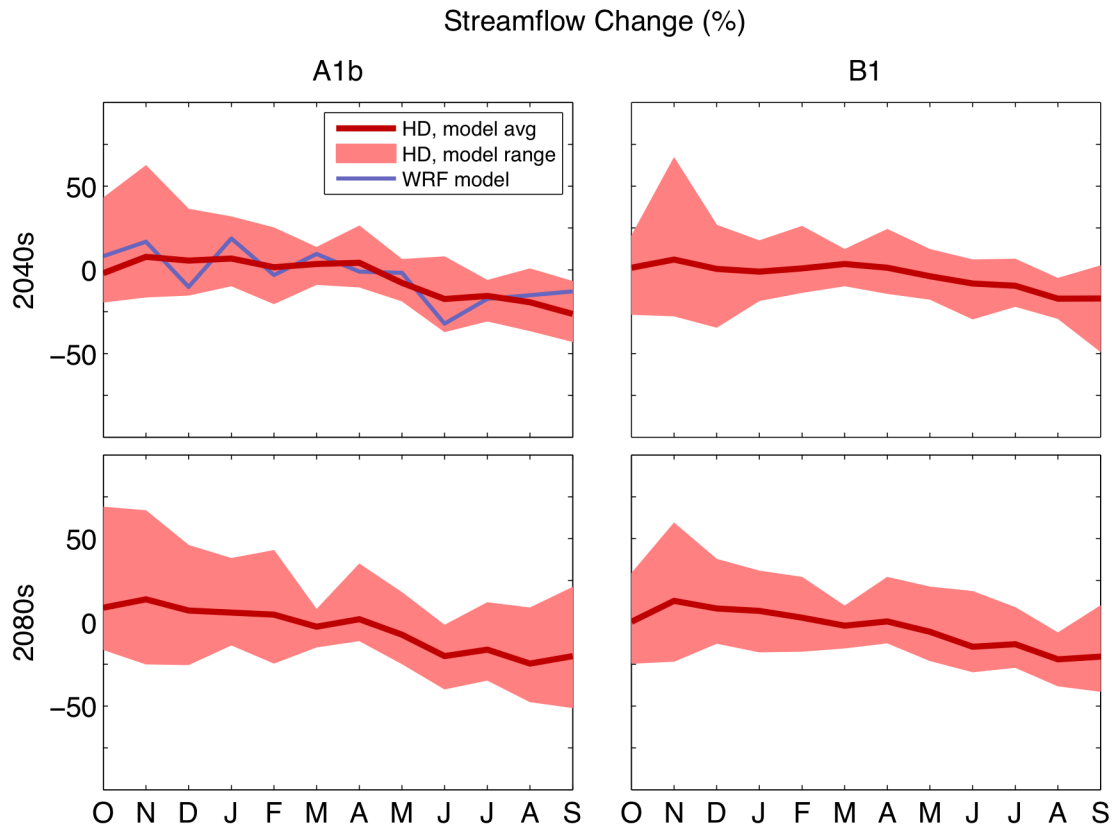

Figure 6. As in Figure 4 but showing projected changes in streamflow (%).

compared to trends through the end of the 21st century. Although the trends are somewhat more distinct for seasonal changes in precipitation – there is a slight tendency towards drier summer and wetter fall, winter, and spring – models disagree on the sign of the change and variability continues to be large through the coming century.

Projected changes in Temperature and Precipitation: Kilchis and Miami basins

Projected changes for the Kilchis and Miami basins largely reflect the trends anticipated for the Pacific Northwest as a whole. Downscaled monthly projections for temperature and precipitation are shown in Figures 4 and 5, respectively. Both figures show the mean projection for all 10 GCMs included in the CBCCSP dataset (thick red line) as well as the minimum and maximum change projected among all 10 models (light red shading). Panels show results for the two emissions scenarios – A1b and B1 – and two future time periods – 2040s and 2080s. In addition to the CBCCSP results, the mean monthly change projected by the WRF regional model is included in the plot of changes for the 2040s A1b scenario. Note that the WRF projection is for the 2050s instead of the 2040s, but that the two averaging periods overlap substantially (2030-2059 vs. 2040-2069).

Consistent with the PNW average projections, these show a pronounced warming that is roughly uniform across all seasons, with a slight tendency towards more

Table 2. Projected changes in monthly mean streamflow for the Kilchis and Miami rivers. Numbers indicate the percent change in flow relative to historical (1970-1999). The range among models (min, max) is shown for the statistically downscaled projections (CBCCSP). Only projections for the A1b emissions scenario are shown.

Month	*CBCCSP, A1b 2040s*	*CBCCSP, A1b 2080s*	*WRF, 2050s*
Jan	-2% (-19 to 43%)	9% (-16 to 69%)	8%
Feb	8% (-16 to 62%)	14% (-25 to 67%)	17%
Mar	5% (-15 to 36%)	7% (-25 to 46%)	-10%
Apr	7% (-9 to 32%)	6% (-13 to 38%)	19%
May	2% (-20 to 25%)	5% (-24 to 43%)	-3%
Jun	3% (-9 to 13%)	-3% (-15 to 8%)	9%
Jul	4% (-10 to 26%)	2% (-11 to 35%)	-1%
Aug	-8% (-19 to 6%)	-7% (-25 to 18%)	-2%
Sep	-17% (-37 to 8%)	-20% (-40 to -2%)	-32%
Oct	-16% (-31 to -6%)	-16% (-34 to 12%)	-17%
Nov	-19% (-36 to 1%)	-25% (-47 to 9%)	-15%
Dec	-26% (-43 to -7%)	-20% (-51 to 21%)	-13%

warming in summer. The spikes in the high end of projected warming from July stem from a particularly warm climate model: HadGEM1 (*Johns et al., 2006*). This model is one of the lowest-performing models among the 10 selected for the CBCCSP project. Precipitation projections are also consistent with PNW-wide changes, showing a large model spread relative to trends, in which the low-end projection is generally of opposite sign to the high-end projection. It is notable that in both cases the WRF projections show very similar trends to that obtained from statistical downscaling. This lends greater confidence in the results, and suggests that – for the Kilchis and Miami basins – important physical processes are not missed by statistically downscaling the GCM projections.

Projected changes in Streamflow: Monthly flows

Monthly projected changes in streamflow (%) for the Kilchis and Miami rivers are shown in Figure 6 (format follows that of Figures 4 and 5). Consistent with the wet, rain-dominant character of these watersheds, these largely reflect the projected

Table 3. Projected changes in several measures of flood severity. All metrics show the change in the magnitude of floods with a specific recurrence interval: 2-, 5-, 50-, and 100-year floods, respectively. Numbers indicate the percent change in flow relative to historical (1970-1999). The range among models (min, max) is shown for the statistically downscaled projections (CBCCSP). Only projections for the A1b emissions scenario are shown.

	Projected Change in Flood Magnitude		
	2-yr	*5-yr*	*50-yr*
CBCCSP, A1b 2040s	8% (-5 to 39%)	9% (-5 to 33%)	13% (-6 to 34%)
CBCCSP, A1b 2080s	17% (-14 to 58%)	16% (-9 to 47%)	25% (3 to 43%)
WRF, A1b 2050s	17%	20%	29%

Table 4. Projected changes in several measures of low flows. The first two columns show results for the 90% and 95% exceedance values for daily flow in each year (p90 and p95, respectively), while the last column shows changes in the magnitude of 7-day low flows with a 10-year return period (7q10). Numbers indicate the percent change in flow relative to historical (1970-1999). The range among models (min, max) is shown for the statistically downscaled projections (CBCCSP). Only projections for the A1b emissions scenario are shown.

	p90	*p95*	*7q10*
CBCCSP, A1b 2040s	-20% (-37 to -11%)	-22% (-37 to -12%)	-20% (-29 to -10%)
CBCCSP, A1b 2080s	-26% (-41 to -16%)	-28% (-41 to -19%)	-24% (-30 to -17%)
WRF, A1b 2050s	-13%	-14%	-10%

changes in precipitation, with a slightly greater tendency towards summer drying, likely a consequence of increased moisture stress in summer. Table 2 lists the percent changes for the A1b scenario, showing a large range among projections, and very few months in which all GCMs agree on the sign of the change in streamflow.

Projected changes in Streamflow: Extremes

Winter flooding and summer low flows are of particular concern for the restoration efforts in the Kilchis and Miami estuaries. Tables 3 and 4 list the projected changes for flooding and low flows, respectively. Changes in flooding are listed for the 2-, 5-, and 50-year recurrence interval of annual peak daily flows. Changes in flooding are projected to be modest, with large variation among model projections. There is a slight tendency towards increases in flooding, though models only agree on the sign of the change for the 50-year floods in the 2080s A1b scenario. Changes in low flows, in contrast, are more robust, with universal model agreement that low flows will decrease in the future. Whereas for flooding the magnitude of changes is greater for more extreme flow metrics (i.e., 50-year flood), all three low flow metrics show approximately the same magnitudes of change.

SEA LEVEL RISE (SLR)

Global Sea Levels: past and future

Sea level is anticipated to rise in response to global warming as a result of thermal expansion of the oceans and melting of land ice. Indeed, observations from tide gauges and satellite data indicate that global sea levels have risen at an average rate of 1.7 ± 0.3 mm/yr during the 20th century and that the rate has been accelerating with time (*Church and White, 2006; IPCC, 2007*; Figure 7).

The relatively recent upward trend in global sea levels is predominantly attributable to three factors (*IPCC, 2007*):

1. Thermal expansion of ocean water as it warms,
2. Contributions from land-based ice as it melts, and

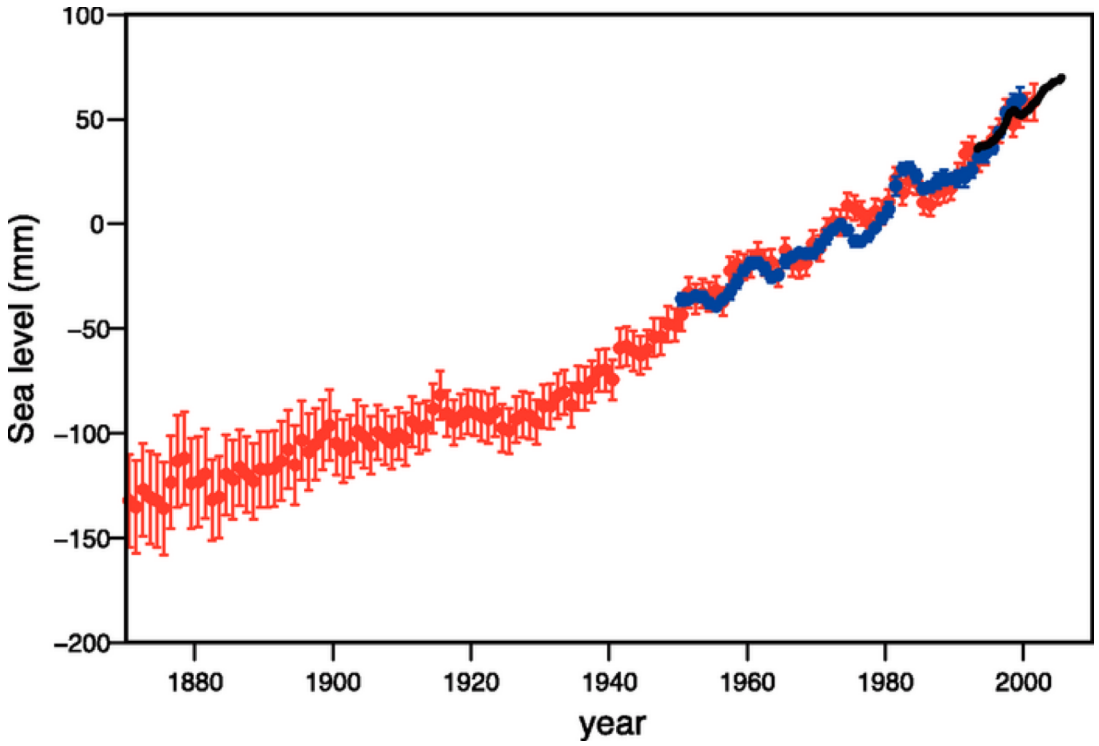

Figure 7. Average annual sea levels. Red dots represent reconstructed sea levels since 1870 with 90% confidence error bars (from *Church and White, 2006*). Blue curve shows coastal tide gauge measurements since 1950 (from *Holgate and Woodworth, 2004*). Black line is based on satellite data (*Leuliette et al., 2004*). *Figure source: IPCC, 2007*.

3. Transmission of terrestrial water storage to the oceans (i.e., withdrawals from aquifers for irrigation that eventually reach the ocean).

Of the three inputs listed, the latter is the most challenging to estimate, though the majority of studies indicate that its net contribution is negligible (*Glick et al., 2012*). For the time period from 1993 to 2007, *Cazenave and Llovel* (*2010*) estimate a global rate of rise of 3.1 ± 0.1 mm/year and that ~30% of the observed rise comes from thermal expansion and ~55% is attributable to the melting of land ice.

In an effort to quantify the fluctuations and to project future changes in global sea levels due to climate change, studies take two approaches: (1) process-based methods and (2) empirical methods. The process-based approach was used by the Intergovernmental Panel on Climate Change (IPCC) in its last assessment (*IPCC, 2007*). These models sum the individual contributors to sea level rise (i.e. thermal expansion of warming water, melting terrestrial glaciers, Greenland and Antarctic melt, etc.) to estimate future sea levels under various scenarios (*Meehl et al., 2007; Solomon et al., 2009*). Empirical methods relate historical global temperature observations to measurements of global sea level, and combine these relationships with global temperature projections to obtain estimates of changes in sea level (e.g., *Rahmstorf, 2007; Vermeer and Rahmstorf, 2009*). Figure 8a (*Moore et al., 2013*) shows that the IPCC's process-based estimates of global SLR are considerably lower than the empirical estimates, in part due to the fact that the IPCC report explicitly

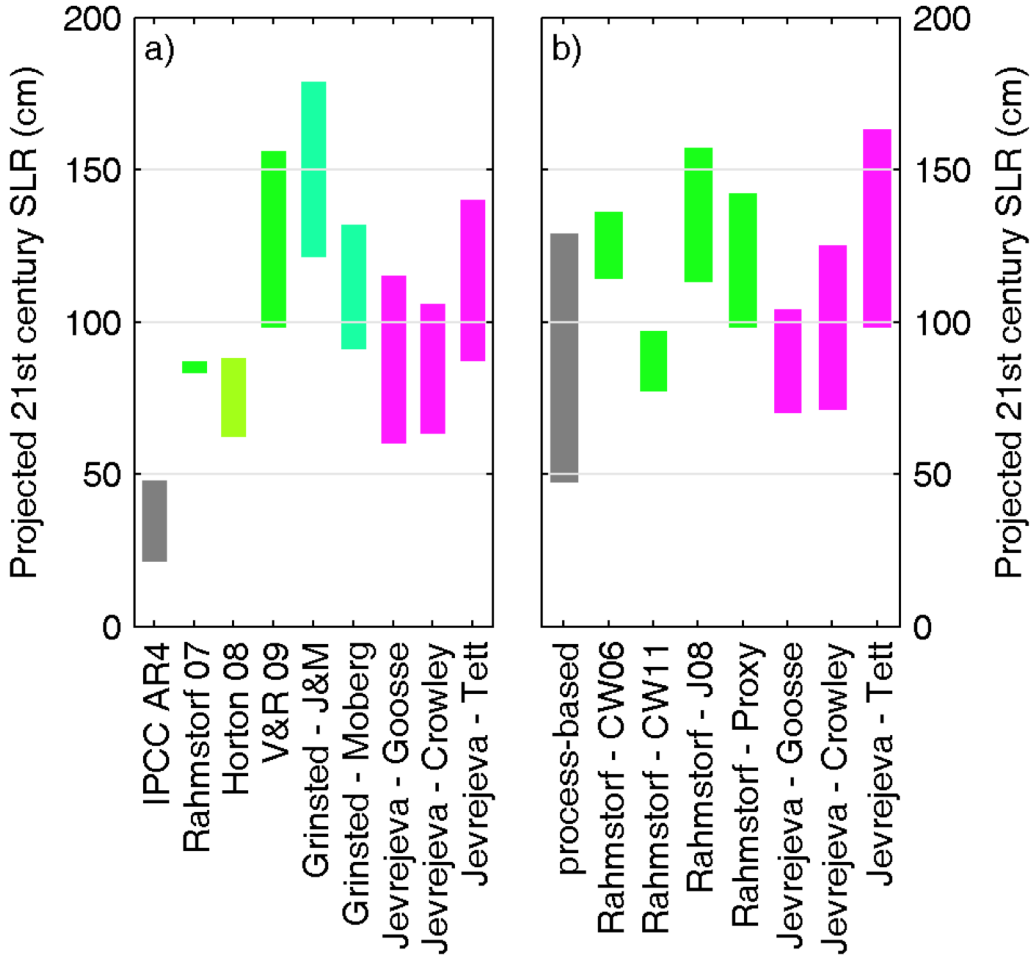

Figure 8. Range of sea level rise projections (5 – 95%) by 2100 from process-based (gray bars) models and semi-empirical (colored bars) models from SRES A1b (a) and RCP8.5 (b). Convergence in b) due to greater uncertainty and upward shift in process-based projections. *Figure source: Moore et al. 2013*.

neglected changes in the rate of melt for the polar ice sheets. Later estimates using process-based approaches, refined to include ice sheet dynamics, are more consistent with semi-empirical results, but have a wider range of uncertainty (Figure 8b).

Regional Contributions to Sea Level Rise

Regionally, sea levels rise and fall in response to complex interactions between ocean characteristics, climate and weather patterns, and geology. Numerous processes can influence local rates of sea level rise, including:

- Atmospheric dynamics
- Large scale climate variations
- Vertical land movement
- Changes in ocean currents

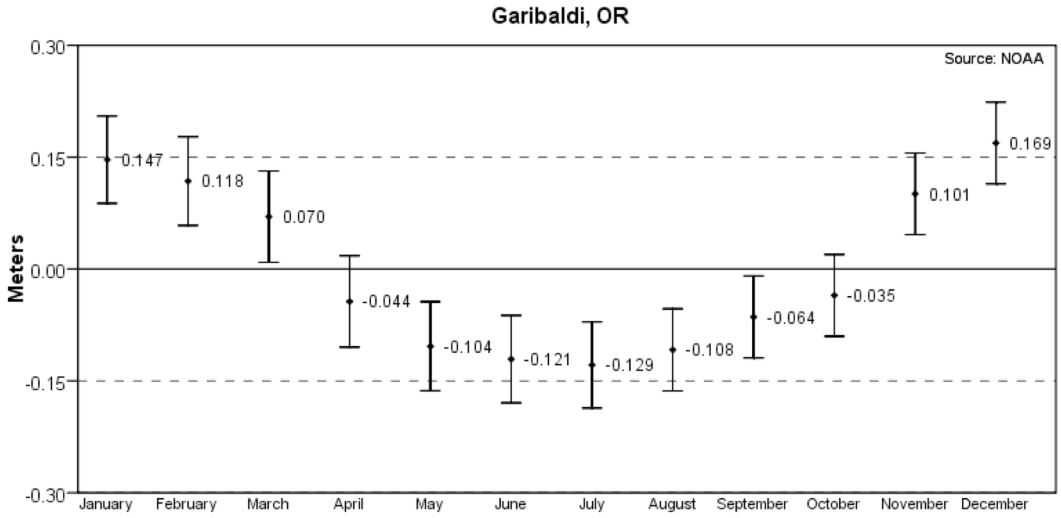

Figure 9. Average seasonal cycle of mean sea levels (with 95% confidence intervals) from NOAA tide gauge at Garibaldi, OR, located at the mouth of the Miami River. Data range is from 1970 to 2013. *Data source:* http://tidesandcurrents.noaa.gov.

Weather patterns affect sea levels via the "inverse barometer" effect, in which sea levels rise in response to decreasing surface pressures and fall in response to the opposite, as well as via the impact of winds on waves and storm surge. Wind direction and strength along the shores of the West Coast vary seasonally, where stronger winds in the winter originate from the southwest and tend to push water against the coast, resulting in higher tides than in the summer when weaker winds emanate from the northwest (*Mote et al., 2008*; Figure 9). Winter higher tides are amplified during El Niño years, which can add up to 30 cm (12") to water levels (*Allan and Komar, 2002, Komar et al., 2011*; Figure 10). El Niño winters also increase wave heights (*Ruggiero et al., 2005*). These changes are associated with the impact of El Niño on wind direction and strength, however large-scale climate variations can also have an impact on water levels via changes in ocean temperatures (e.g., *Bromirski et al., 2011*). Vertical land movement can either accelerate or decelerate the local manifestation of sea level rise. Land subsidence and uplift can occur as a result of ongoing tectonic activity, such as along the Cascadia subduction zone (Figure 9), or due to an ongoing response of the earth's crust to the recession of ice since the last ice age (so-called "isostatic rebound"). Finally, changing ocean currents can affect the rate of local rates of sea level rise, since surface currents in particular are accompanied by gradients in sea surface height.

The influence of vertical land movement is particularly important along the U.S. West coast, with the sign and magnitude of uplift varying substantially along the coast. Overall, the California coast south of Cape Mendocino is predominantly subsiding, enhancing sea level rise, and the coastal areas of to the north are generally uplifting, either partially or completely offsetting the effects of sea level rise. However at a finer resolution, there is considerable variability of vertical land

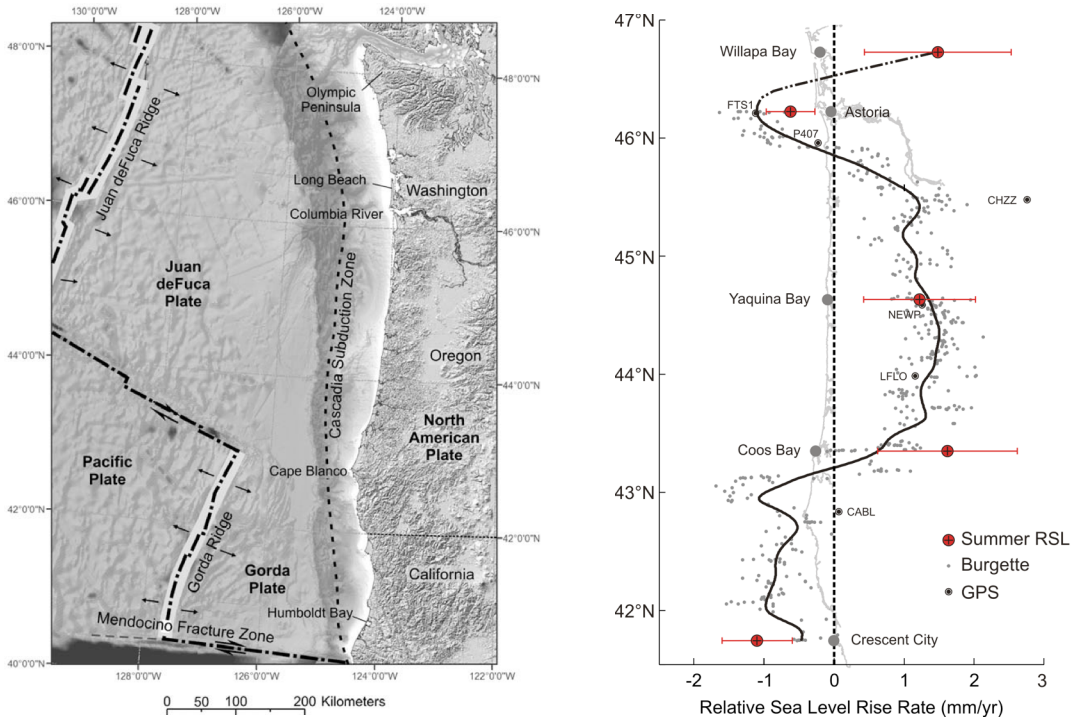

Figure 10. Tectonic landscape of the Pacific Northwest (left); and relative change in sea level along the Oregon coast (right) based on analysis of NOAA tide gauges (red circle crosshairs with 95% confidence bars) combined with land elevation change data from benchmark surveys (grey dots) and GPS measurements (black dots). Values are for summer months only to account for the effects of ENSO (right). *Figure source: Komar et al. 2011*.

movement along the coast north of Cape Mendocino. The Oregon coast demonstrates considerable variability in both the sign and magnitude of vertical land motion, with sharp changes occurring even over short distances (Figure 10; *Komar et al., 2011*). A further complications is that as land-based ice melts, the gravitational attraction between the ice sheet and proximate ocean diminishes; and the surrounding Earth's crust deforms in response to the ice load re-distribution (*Mitrovica et al. 2009*). This phenomenon, known as "sea level fingerprinting," is projected to reduce relative sea levels along the northern U.S. West Coast, including the Tillamook Bay area (*Glick 2012*).

The National Oceanic and Atmospheric Administration (NOAA) maintains a tide gauge at Garibaldi, near the mouth of the Miami River. Based on observations at Garibaldi from 1970 to present, the Miami river has experienced a rise of 1.98 ± 1.82 mm/yr (Figure 11). However, the paucity of observations makes this trend estimate unreliable. In an in-depth assessment combining tide gauge data from multiple points along the coast and accounting for vertical land movement, *Burgette et al.* (*2009*) find a rate of sea level rise of 0.88 (±0.08) mm/yr at Garibaldi for the time period 1925 – 2006.

Regional Projections of Sea Level Rise

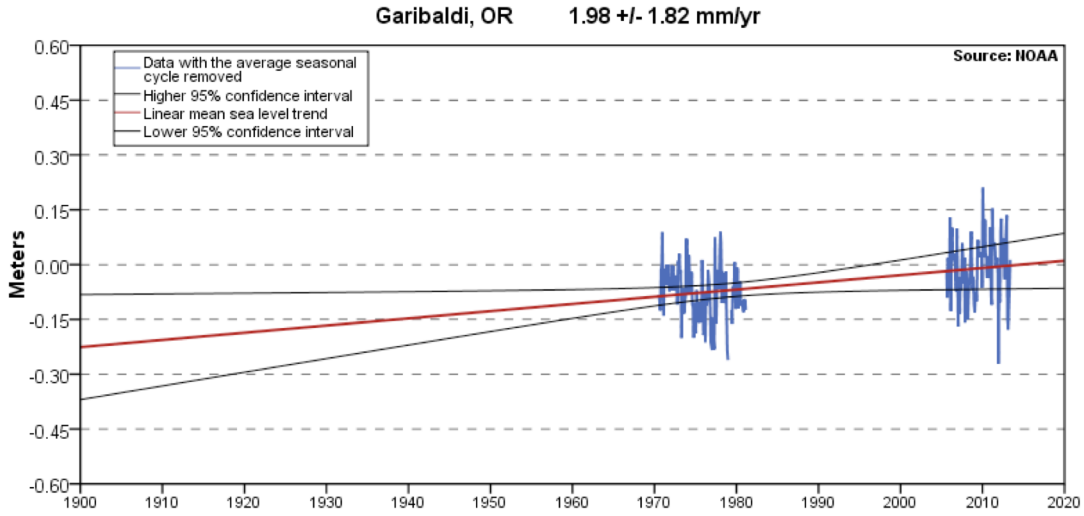

Figure 11. Monthly mean sea levels (blue lines) with the seasonal fluctuations (currents, temperatures, winds, atmospheric pressures) removed for 1970 to 2013. Note the substantial amount of missing data. Long-term linear trend is shown in red with 95% confidence intervals (black lines). *Data source:* http://tidesandcurrents.noaa.gov

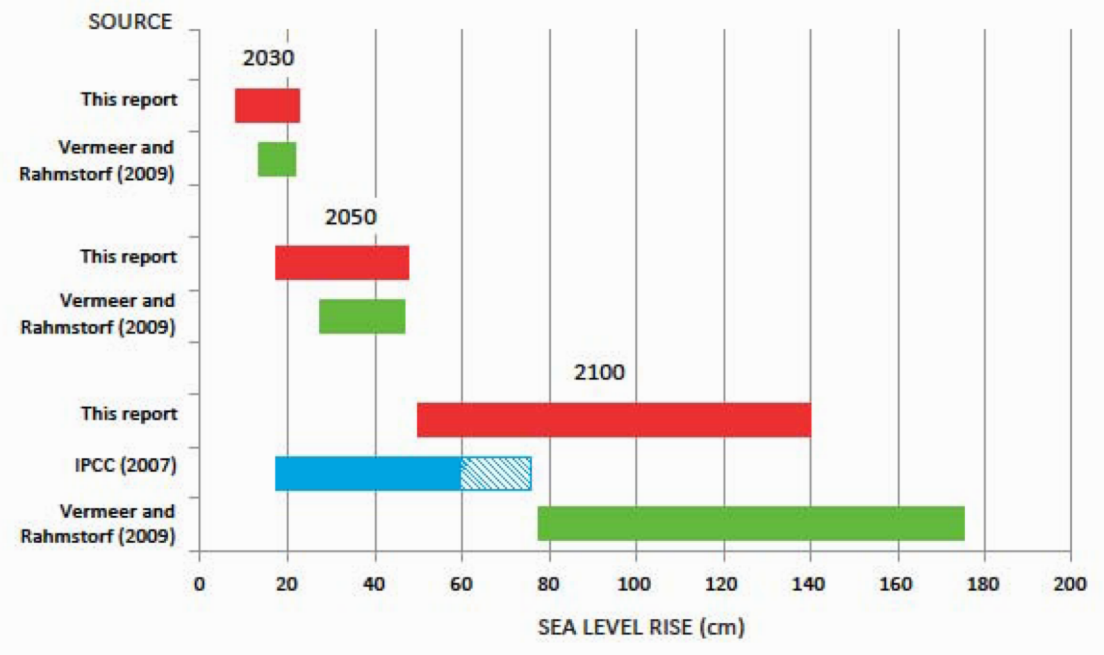

Figure 12. Projection of global sea level rise from three sources for 2030, 2050 and 2100. "This report" projections refer to *NRC, 2012* (the source of this figure). The hatched blue lines in the IPCC's 2100 projections represent scaled-up ice sheet discharge estimated after the report was released in 2007.

Most studies of regional sea level rise use the process-based estimates of global SLR from the IPCC (*2007*) and then add (or subtract) the regional factors contributing to variations in relative sea levels (e.g., *Mote et al., 2008*). Among the most

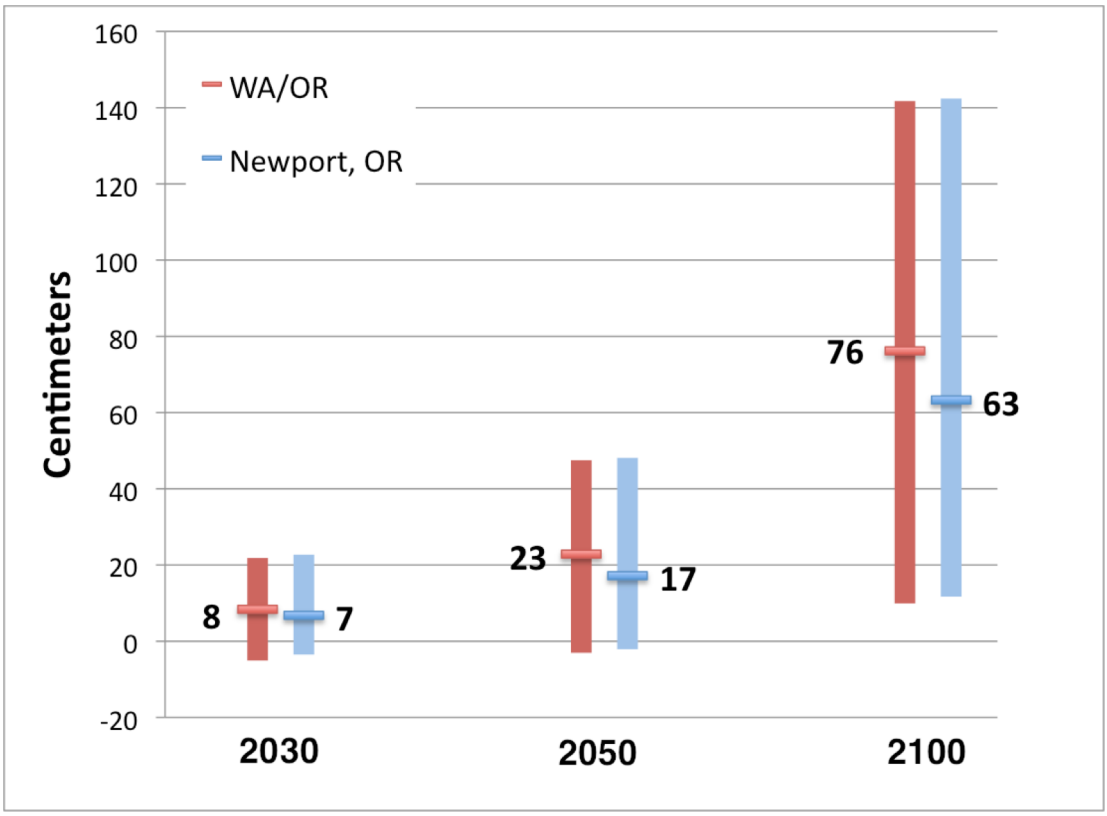

Figure 13. SLR projections for Washington and Oregon and for Newport, OR estimated by the NRC based on global models from the IPCC and regional factors contributing to relative sea level rise. The range of projections represents the highest and lowest emissions scenarios and the horizontal lines (and associated numbers) indicate estimates from the mid-range scenario (A1b). Values are for the estimated sea level relative to the year 2000. *Figure based on data from Glick (2012).*

comprehensive of these is the synthesis recently published by the National Research Council (NRC) in 2012 (*Glick et al., 2012)*, examining SLR along the West Coast of the conterminous U.S. The NRC updated IPCC's (*2007*) process-based global estimates by re-calculating projected sea level changes due to thermal expansion and extrapolating land-based ice melt from observations. The updated global estimates were compared to calculations from empirical models (*Vermeer and Rahmstorf, 2009*) to validate the values. Figure 12 illustrates how the projections compare among the various modeling techniques applied to three future time periods: 2030, 2050, and 2100 (projections from IPCC are shown only for the last time period).

With the updated, re-calculated global projections for SLR, the NRC estimated regional contributions to relative sea levels at various locations along the coasts of California, Oregon and Washington. An overarching pattern underscored by the NRC report is the general tectonic setting of uplift in coastal areas north of Cape Mendocino, CA, which partially offsets regional SLR estimates. Accounting for the regional factors mentioned above in this report, the NRC estimated the relative SLR for Oregon and Washington and also at a finer resolution at several sites including Newport, OR (the most proximate site to Tillamook Bay). Figure 13 shows these

projections for the three future time periods, where the range represents the estimates from the lowest (B1) to the highest (A1FI) the greenhouse gas emissions scenarios (Nakićenović, 2000); the results for regional SLR are also listed in Table 5.

Table 5. As in Figure 13, SLR projections estimated by the NRC. *Data source: Glick* (*2012*).

	Location	
Year	*WA/OR*	*Newport, OR*
2030	8 (-5 to 22)	7 (-4 to 23)
2065	23 (-3 to 47)	17 (-2 to 48)
2100	76 (10 to 142)	63 (12 to 142)

The estimates reported by the NRC are comparable to those developed by Climate Central, an independent research group that conducts peer-reviewed syntheses and studies on climate change and its projected impacts. In March of 2012, Climate Central completed a review of sea level rise and the impacts to all coastal states in the U.S. (*Strauss et al., 2012*). Applying a similar methodology as the NRC study, they used empirical estimates of global SLR (*Tebaldi et al., 2012*) combined with regional factors and provide estimates at very fine spatial scales along the coast. These include estimates for Oregon sites at Charleston (Coos Bay), South Beach (Yaquina River) and Astoria (Tongue Point) (Table 6).

Finally, we note that – in addition to the fact that the Kilchis and Miami estuaries are likely sheltered wave action – current research indicates that storm surge will not change significantly with global warming (e.g., *Hamman, 2012*). However, the combination of higher water levels associated with SLR and storm surge events is projected to make previous 100-year flood event occur more frequently. *Tebaldi et al.* (*2012*), for instance, project that 100-year extreme sea levels along the Oregon coast will occur with a 5-year return interval by 2050 (i.e., these events will increase from a 1% to a 20% probability of occurrence).

SUMMARY

Sea level rise and streamflow change projections are needed to inform restoration actions at the Kilchis site and evaluate the effectiveness of existing restoration at the Miami river site. Previous sections in this report present the results of an analysis of CIG projections of changes in climate and streamflow in the Kilchis and Miami basins as well as a review of the research on past and future sea level rise for the region.

Projected changes in temperature show a clear warming signal that is outside of the range of natural variability. This is contrasted by projections of precipitation that show small trends relative to

Table 6. Localized SLR projections from Climate Central's Surging Seas report (*Strauss et al., 2012*). Values are in cm of rise over the period 2009-2050, with the 90% confidence limits in parentheses.

Site	*Nearest city*	*Projected SLR*
Coos Bay	Charleston, OR	23 (51-508)
Yaquina River	South Beach, OR	30 (13- 56)
Tongue Point	Astoria, OR	18 (0- 46)

year-to-year fluctuations in climate. Evaluating simulations of streamflow we find reasonable agreement with nearby flow measurements (Nash-Sutcliffe: 0.6, correlations ranging from 0.4-0.8). Projected changes in streamflow are consistent with expectations for warm, rain-dominant basins such as these: changes are predominantly driven by variations in precipitation: warmer temperatures only have a slight effect on summer flows via their impact on evaporative demand. GCMs disagree on the sign of trends in streamflow for nearly all months and emissions scenarios through the end of the 21st century. Although models disagree on the sign of the trend, the central tendency is for decreasing flows in spring and fall and increasing flows in fall and winter. Apart from the warmest scenario and the most extreme floods (change in 50-year flood for A1b 2080s), models also disagree on the sign of the trends in flooding. Here again, despite disagreement, there is a modest tendency towards increasing flood magnitudes for all flood metrics. In contrast with the other streamflow metrics, models are in universal agreement that low flow extremes will become more severe with warming, projecting a decrease of 20-28% depending on the metric and future time period.

Local rates of sea level rise are driven by changes in ocean temperatures and currents, terrestrial storage of water and ice, the global distribution of ice melt, vertical deformation of the earth's crust, and by the pattern and intensity of weather patterns. Global estimates of sea level rise indicate a 20th century rate of 1.7 ± 0.3 mm/yr (*Church and White, 2006, IPCC 2007*) and find evidence for a near-doubling of this rate in recent decades. Globally, thermal expansion of the oceans contributes about one-third of the current rise in sea level, while the remaining fraction is predominantly due to melting land ice. Although the literature on sea level rise is quite well-developed for global and regional estimates of sea level rise, few robust, local estimates exist for the PNW. This is predominantly do to the difficulty of estimating local sea level rise in a region as tectonically active as the Northwest, were large variations in both the direction and magnitude of vertical land motion can occur over very short distances. Future projections are also hampered by the lack of detail in estimates of vertical land motion. Nevertheless, the regionally averaged projections for the Pacific Northwest are much larger than potential rates of land uplift by the end of the 21st century, with sea levels estimated to be from 18-140 cm higher than in the year 2000.

REFERENCES

Allan, J. C. and P. D. Komar. (2002): *Extreme storms on the Pacific Northwest Coast during the 1997-98 El Niño and 1998-99 La Niña.* Journal of Coastal Research, 18, 175-193.

Bromirski, P. D., Miller, A. J., Flick, R. E., & Auad, G. (2011): *Dynamical suppression of sea level rise along the Pacific coast of North America: Indications for imminent acceleration.* Journal of Geophysical Research: Oceans (1978–2012), 116(C7).

Burgette, R. J., R. J. Weldon II, and D. A. Schmidt (2009): *Interseismic uplift rates for*

western Oregon and along-strike variation in locking on the Cascadia subduction zone, J. Geophys. Res., 114, B01408, doi:10.1029/2008JB005679.

Cazenave, A. and Llovel, W. (2010): *Contemporary sea level rise.* Annual Review of Marine Science, 2: 145 – 73. DOI: 10.1146/annurev-marine-120308-081105.

Christensen, J. H., Boberg, F., Christensen, O. B., & Lucas-Picher, P. (2008): *On the need for bias correction of regional climate change projections of temperature and precipitation.* Geophysical Research Letters, *35*(20)

Church, J.A. and White, N.J. (2006): *A 20th century acceleration in global sea-level rise.* Geophysical Research Letters, 33. DOI: 10.1029/2005GL024826.

Daly, C., R. P. Neilson, and D. L. Phillips, 1994: A Statistical-Topographic Model for Mapping Climatological Precipitation over Mountainous Terrain. *Journal of Applied Meteorology*, **33**, 140-158.

Daly, C., W. P. Gibson, G. Taylor, G. L. Johnson, and P. Pasteris, 2002: A knowledge-based approach to the statistical mapping of climate. *Climate Research*, **22**, 99-113.

Dulière, Valérie, Yongxin Zhang, Eric P. Salathé, (2011): *Extreme Precipitation and Temperature over the U.S. Pacific Northwest: A Comparison between Observations, Reanalysis Data, and Regional Models*. J. Climate, **24**, 1950–1964. doi: http://dx.doi.org/10.1175/2010JCLI3224.1

Gao, Huilin, Qiuhong Tang, Xiaogang Shi, Chunmei Zhu, Ted Bohn, Fengge Su, Justin Sheffield, Ming Pan, Dennis Lettenmaier, and Eric F. Wood (2009). *Water Budget Record from Variable Infiltration Capacity (VIC) Model Algorithm Theoretical Basis Document.* Dept. Civil and Environmental Eng., Univ. Washington, Seattle, WA: 09-18.

Glick, P., J. Clough, and B. Nunley (2007): *Sea-level Rise and Coastal Habitats in the Pacific Northwest: An Analysis for Puget Sound, Southwestern Washington, and Northwestern Oregon*. National Wildlife Federation, 94. http://www.nwf.org/sealevelrise/pdfs/PacificNWSeaLevelRise.pdf

Hamlet, A. F. and D. P. Lettenmaier (2005): Production of Temporally Consistent Gridded Precipitation and Temperature Fields for the Continental United States. *Journal of Hydrometeorology*, **6**, 330-336.

Hamman, J. (2012): *Effects of Projected Twenty-First Century Sea Level Rise, Storm Surge, and River Flooding on Water Levels in Puget Sound Floodplains and Estuaries.* Master's Thesis for Civil and Environmental Engineering – University of Washington.

Hosking, J. R. M. (1990): *L-moments: Analysis and estimation of distributions using linear combinations of order statistics,* J. R. Stat. Soc., Ser. B, 52*(2),* 105–124.

Hosking, J. R. M., & Wallis, J. R. (1993): *Some statistics useful in regional frequency analysis.* Water Resources Research, *29*(2), 271-281.

IPCC (2001): *Climate Change 2001: The Scientific Basis. Contribution of Working Group I to the Third Assessment Report of the Intergovernmental Panel on Climate Change* [Houghton, J.T., Y. Ding, D.J. Griggs, M. Noguer, P.J. van der Linden, X. Dai, K. Maskell, and C.A. Johnson (eds.)]. Cambridge University Press, Cambridge, United Kingdom and New York, NY, USA, 881pp.

IPCC (2007): *Climate Change 2007: The Physical Science Basis. Contribution of Working Group I to the Fourth Assessment Report of the Intergovernmental Panel*

on Climate Change [Solomon, S., D. Qin, M. Manning, Z. Chen, M. Marquis, K.B. Averyt, M.Tignor and H.L. Miller (eds.)]. Cambridge University Press, Cambridge, United Kingdom and New York, NY, USA.

Kimball JS, Running SW, Nemani R (1997): *An improved method for estimating surface humidity from daily minimum temperature.* Agr Forest Meteorology 85(1-2):87–98

Knutti, R., D. Masson, and A. Gettelman (2013), *Climate model genealogy: Generation CMIP5 and how we got there,* Geophys. Res. Lett., 40, 1194–1199, *doi:*10.1002/grl.50256.

Komar, P.D., Allan, J.C., Ruggerio, P. (2011): *Sea level variations along the U.S. Pacific Northwest Coast: Tectonic and climate controls.* Journal of Coastal Research, 27(5): 808 – 823. DOI: 10.2112/JCOASTRES-D-10-00116.1.

Leung, L. R., and Y. Qian (2009): *Atmospheric rivers induced heavy precipitation and flooding in the western U.S. simulated by the WRF regional climate model.* Geophys. Res. Lett., **36**.

Liang, X., D. P. Lettenmaier, E. F. Wood, and S. J. Burges (1994): A simple hydrologically based model of land surface water and energy fluxes for general circulation models. J. Geophys. Res, **99**, 14,415-14,428.

Littell, J.S., M.M. Elsner, G. S. Mauger, E. Lutz, A.F. Hamlet, and E. Salathé (2010): *Regional Climate and Hydrologic Change in the Northern US Rockies and Pacific Northwest: Internally Consistent Projections of Future Climate for Resource Management.*

Maurer, E. P., A. W. Wood, J. C. Adam, D. P. Lettenmaier, and B. Nijssen (2002): *A Long-Term Hydrologically Based Dataset of Land Surface Fluxes and States for the Conterminous United States*. Journal of Climate, **15**, 3237-3251.

Meehl, G. A., C. Covey, T. Delworth, M. Latif, B. McAvaney, J. F. B. Mitchell, R. J. Stouffer, and K. E. Taylor (2007): The WCRP CMIP3 multi-model dataset: A new era in climate change research,*Bulletin of the American Meteorological Society,* **88**, 1383-1394.

Mitrovica J.X., Gomez N., Clark P.U. (2009): *The sea-level fingerprint of West Antarctic collapse.* Science 323:753

Moore, J.C., Grinsted, A., Zwinger, T., Jevrejeva, S. (2013): *Semi-empirical and process-based global sea level projections.* American Geophysical Union. DOI: 10.1002/rog.20015.

Mote, P., Petersen, A., Reeder, S., Shipman, H., Whitely Binder, L.C. (2008): *Sea level rise in the coastal waters of Washington State.* Report prepared by the Climate Impacts Group, Center for Science in the Earth System, Joint Institute for the Study of the Atmosphere and Oceans, University of Washington, Seattle, Washington and the Washington Department of Ecology, Lacey, Washington.

Nakićenović N, Swart R (eds.) (2000) *Special report on emissions scenarios.* A special report of working group III of the Intergovernmental Panel on Climate Change. Cambridge University Press, Cambridge, United Kingdom and New York, NY, USA, 599 pp.

Neiman, P. J., L. J. Schick, F. M. Ralph, M. Hughes, and G. A. Wick (2011): *Flooding in western Washington: The connection to atmospheric rivers*. J. Hydrometeor., 12, 1337–1358.

Rahmstorf, S. (2007): *A semi-empirical approach to projecting future sea-level rise*, Science, 315, 368-370.

Roeckner, E., L. Bengtsson, J. Feichter, J. Lelieveld, and H. Rodhe (1999): *Transient climate change simulations with a coupled atmosphere-ocean GCM including the tropospheric sulfur cycle.* J Climate, **12,** 3004-3032.

Roeckner, E. et al. (2003): *The atmospheric general circulation model ECHAM5, Part I: Model description*, Max-Planck-Institute for Meteorology Report No. 349.

Ruggiero, Peter; Kaminsky, George M.; Gelfenbaum, Guy; Voigt, Brian (2005): Seasonal to interannual morphodynamics along a high-energy dissipative littoral cell. Journal of Coastal Research. Vol. 21 Issue 3, p553-578. 26p. DOI: 10.2112/03-0029

Salathe E.P., Leung L.R., Qian Y., and Zhang YX. (2010): *Regional climate model projections for the State of Washington*. Climatic Change, 102: 51-75.

Salathé, E. P., A. F. Hamlet, M. Stumbaugh, S.-Y. Lee, R. Steed (2013): *Estimates of 21st century flood risk in the Pacific Northwest based on regional climate model simulations.* Water Resources Research (in review).

Shepard, D. S. (1984): Computer mapping: The SYMAP interpolation algorithm. in *Spatial Statistics and Models*, G. L. Gaille and C. J. Willmott, Eds., Reidel, 133-145.

Snover, A. K., N. J. Mantua, J. S. Littell, M. A. Alexander, M. M. McClure (2013): *Choosing and using climate change scenarios for ecological impacts and conservation decisions.* Conservation Biology (in press).

Solomon, S., Plattner, G., Knutti, R., and P. Friedlingstein (2009): Irreversible climate change due to carbon dioxide emissions, Proc Natl Acad Sci USA, 106, 1704-1709.

Stedinger, J. R., R.M. Vogel, and E. Foufoula-Georgiou, 1993. Frequency analysis of extreme events. Handbook of Hydrology, D. R. Maidment, ed., McGraw-Hill, Inc, New York.

Strauss, B., Tebaldi, C., Ziemlinski, R. (2012): Surging Seas: Sea level rise, storms, and global warming's threat to the U.S. coast. A Climate Central Report http://slr.s3.amazonaws.com/SurgingSeas.pdf

Tebaldi, C., Strauss, B.H., Zervas, C.E. (2012): Modelling sea level rise impacts on storm surges along US coasts. Environmental Research Letters. doi:10.1088/1748-9326/7/1/014032

Thornton PE, Running SW (1999): *An improved algorithm for estimating inci- dent daily solar radiation from measurements of temperature, humidity, and precipitation.* Agr Forest Meteorology 93(4):211–228

Vermeer, M., and S. Rahmstorf (2009): *Global sea level linked to global temperature.* Proceedings of the National Academy of Sciences of the United States of America, 106(51), 21527-21532.

Wang QJ (1997): *LH moments for statistical analysis of extreme events.* Water Resour. Res., 33(12):2841-2848.

Warner, M. D., Mass, C. F., & Salathé Jr, E. P. (2012): *Wintertime Extreme Precipitation Events along the Pacific Northwest Coast: Climatology and Synoptic Evolutio*n. Monthly Weather Review, *140*(7), 2021-2043.

Wood, A. W., Leung, L. R., Sridhar, V., & Lettenmaier, D. P. (2004): *Hydrologic implications of dynamical and statistical approaches to downscaling climate model outputs*. Climatic change, *62*(1-3), 189-216.

Zhang, Y., Dulière, V., Mote, P. W., & Salathé Jr, E. P. (2009): *Evaluation of WRF and HadRM Mesoscale Climate Simulations over the US Pacific Northwest*. J. Climate, *22*(20), 5511-5526.

Zhao, R., R. Zhuang, L. Fang, X. Liu, and Q. Zhang (1980): *The Xinanjiang model*. International Association of Hydrological Sciences, Publ. No. 129, pp. 351–356

APPENDIX: Additional background on the methodology

This appendix is intended to supplement the *Data & Methods* section by providing additional background and detail regarding the development of the downscaled streamflow projections. References are also provided for additional reading.

Global Climate Models (GCMs) and Emissions Scenarios

Future greenhouse gas emissions are needed to estimate changes in climate beyond the middle of the 21st century (near-term climate change is primarily affected by past emissions). To do so, greenhouse gas emissions scenarios – "what if" scenarios about future emissions – are used as estimates of possible future emissions. Since we do not know a priori how global emissions will unfold in the future, these are termed scenarios. Likewise, global model simulations that are based on these scenarios are termed "projections," since they are distinct from forecasts or predictions. The emissions scenarios used in this report stem from the Special Report on Emissions Scenarios (SRES; *Nakićenović et al., 2000*). Specifically, we use the A1b and B1 emissions scenarios. The B1 is a low-end estimate of future emissions, while the A1b is a medium estimate of 21st century emissions.

GCMs are sophisticated numerical representations of the processes affecting the Earth's climate. Coupling atmosphere, ocean, and land models, GCMs simulate the interactions among these and the implications for changing temperature, precipitation, and other climate variables. GCMs perform well across a variety of metrics (e.g., *Knutti et al., 2013*), including good fidelity to 20th century variations in temperature, and newer model versions have improved measurably over time. The GCM projections used in this report all stem from the World Climate Research Programme (WCRP) Coupled Model Intercomparison Project, Phase 3 (CMIP3; *Meehl et al, 2007*).

Downscaling

Since GCMs have a low spatial resolution – often with a spacing of 100-200 km between grid cells – they do not resolve many of the important small-scale processes that are important in management applications. The term "downscaling" refers to methods that are developed to bridge the gap between the coarse spatial resolution of GCMs and the finer-scale details that are relevant to decision-making. There are two general approaches to downscaling: statistical and dynamical. Statistical methods relate observationally-based climate information (e.g., from weather stations) to changes projected by GCMs, thereby combining fine-scale detail from observations with large-scale projections from the global models. Dynamical downscaling, in contrast, is a physics-based approach in which a Regional Climate Model (RCM) is run with GCM projections as a boundary condition. Because the RCM is run over a smaller region, it can be implemented at a finer resolution. As a result, RCMs have the potential to resolve fine-scale processes that are unresolved by GCMs

and therefore not captured via statistical downscaling[1]. The primary disadvantage of dynamical downscaling is that it is expensive to implement, meaning that there are generally fewer realizations and therefore less robust estimates of projected change. Statistical downscaling, in contrast, is quite simple to apply and therefore more feasible to use in producing a large ensemble of downscaled climate projections from different GCMs and emissions scenarios. For a concise summary of the advantages and disadvantages of each, see Appendix C of *WHCWG (2013)*.

Gridded Meteorological Dataset

Both the statistically and dynamically downscaled projections used in this project were adjusted using a gridded historical dataset based on observations obtained from surface weather stations. The dataset was produced as part of the CBCCSP project, and is described in detail by *Hamlet et al. (2010).* It consists of daily values for precipitation, maximum and minimum temperature, and surface wind, gridded at a spatial resolution of 1/16th degree (0.0625-degree) for the years 1915 through 2006.

To construct the dataset, National Climatic Data Center (NCDC) Cooperative Observer (COOP) network stations are queried to incorporate stations having at least 5 years of data and at least 365 days of continuous observations. Selected stations are then regridded to the 0.0625-degree grid using the Symap algorithm which uses an inverse-distance weighting of the 4 nearest neighbor s reporting on a given day (*Shepard, 1984; Maurer et al., 2002; Hamlet and Lettenmaier, 2005*). The station network configuration evolves throughout the available record and therefore monthly time-step U.S. Historical Climatology Network (HCN) stations are used to correct temporal biases and shifts arising from network changes. The Precipitation Regression on Independent Slopes (PRISM; *Daly et al., 1994; 2002*) monthly normals are then aggregated from a regular 30 arc-second grid to the 0.0625-degree grid and subsequently used to scale precipitation and mean temperature, to the PRISM calendar month climatology—improving representation of orographic influences and minimizing observing network biases.

Note that the gridded historical dataset is produced by combining surface meteorological observations with assumptions regarding the impact of terrain features (elevation, exposure, etc.) on temperature and precipitation in order to interpolate these onto the output grid. In remote and topographically complex regions, the terrain-based assumptions can result in biases in the gridded product, and these biases can vary with meteorology and season. At larger scales – as defined

[1] An example is the interaction between soil moisture and warming: with greater warming comes greater risk of water stress and, ultimately, depletion of water stored in the soil column. Soil moisture depletion is often associated with accelerated warming, since the moisture can no longer buffer heat events through evaporation. GCMs may not be able to adequately represent spatial variability in soil moisture resulting from variations in elevation, exposure, and vegetation cover. RCMs, though imperfect as well, have the potential to more accurately represent small-scale mechanisms such as these.

by the density of surface observations from which the gridded product is produced – we can be confident that the gridded observations are a good approximation. Similarly, averages over longer time periods are likely to be more accurate. However, biases are likely to increase with decreasing spatial scale, and could be important in areas with complex terrain and sparse observations.

Hydrologic Simulations

The final gridded dataset – including both historical climate and downscaled GCM projections – is used as input to the Variable Infiltration Capacity (VIC) hydrologic model (*Liang et al., 1994; Gao et al., 2010*) to estimate past and future hydrologic conditions in the basin. VIC calculates the sensible and latent heat fluxes according to physical formulations, but it uses conceptual schemes to represent the surface runoff and base flow. What makes the VIC model unique is its representation of the soil column and parameterization of the infiltration process, which impacts the vertical distribution of soil moisture in the model grid cell. The VIC model represents multiple vegetation types and soil layers, which allows for variable infiltration and evaporation. The infiltration and surface runoff scheme follows the Xinanjiang model (*Zhao et al., 1980*), in which infiltration follows a non-linear relationship and which allows for an interflow component that represents water that is neither surface runoff nor immediately recharged to groundwater. Three parameters describe the shape of the infiltration capacity curve and these are generally defined through VIC model calibration.

VIC is driven by daily inputs of precipitation, maximum and minimum air temperature, and wind speed. Additional model forcings that drive the water and energy balance, such as solar (shortwave) and longwave radiation, relative humidity, vapor pressure and vapor pressure deficit, are calculated in a pre-processing step within the model. The forcings preprocessor follows algorithms developed by *Thornton and Running (1999)* and *Kimball et al. (1997)*.